THE JOURNAL OF PHYSICAL CHEMISTRY LETTERS
A JOURNAL OF THE AMERICAN CHEMICAL SOCIETY

pubs.acs.org/JPCL

Perspective

Advancing Organic Photoredox Catalysis: Mechanistic Insight through Time-Resolved Spectroscopy

Vanessa M. Huxter*

Cite This: J. Phys. Chem. Lett. 2024, 15, 7945−7953

Read Online

ACCESS | Metrics & More | Article Recommendations

ABSTRACT: The rapid development of light-activated organic photoredox catalysts has led to the proliferation of powerful synthetic chemical strategies with industrial and pharmaceutical applications. Despite the advancement in synthetic approaches, a detailed understanding of the mechanisms governing these reactions has lagged. Time-resolved optical spectroscopy provides a method to track organic photoredox catalysis processes and reveal the energy pathways that drive reaction mechanisms. These measurements are sensitive to key processes in organic photoredox catalysis such as charge or energy transfer, lifetimes of singlet or triplet states, and solvation dynamics. The sensitivity and specificity of ultrafast spectroscopic measurements can provide a new perspective on the mechanisms of these reactions, including electron-transfer events, the role of solvent, and the short lifetimes of radical intermediates.

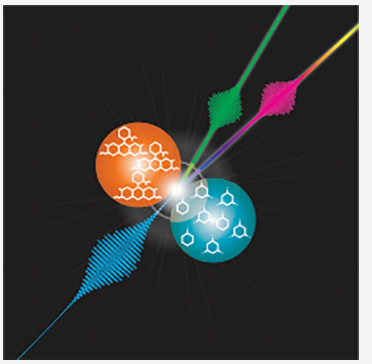

Photoredox catalysis has enabled researchers to overcome previously intractable problems in organic synthesis,[1,2] natural product synthesis,[3] and the synthesis of pharmaceuticals.[4] Advancements in chemical synthetic methods achieved by light-activated techniques have made challenging chemical reactions possible across a wide variety of substrates. The use of light to drive reactions has allowed for more selective reactions that generate both simple and complex molecules from renewable and economic starting materials under mild conditions. In addition, photoredox catalysis corresponds to many of the broadly defined principles of green chemistry.[5,6] Using light excitation, photoredox catalysis can initiate single electron-transfer processes to drive chemical reactions starting from generally inert or stable reactants. This means that activation with harsh or toxic synthetic methods is not required to permit highly endothermic and selective reactions, leading to safer conditions.

The term photocatalysis first appeared in the literature in the early 1900s.[7] Much of the early work on photoredox catalysis focused on transition metal coordination compounds with charge transfer bands, e.g., tris(2,2′-phenylpyridine) iridium or tris(2,2′-bipyridine) ruthenium(II) ($Ru(bpy)_3$). An early report of $Ru(bpy)_3$ as a photocatalyst dates to 1978.[8] In addition to the widely used inorganic complexes, organic chromophores have been highly successfully as photocatalysts due to their potentially strong reactivity and wide diversity, including eosin y and methylene blue[9] dyes. The modern era of photoredox catalysis began in 2008 with simultaneous papers from Yoon et al.[10] and MacMillan et al.[11] Both used $Ru(bpy)_3$ to either drive [2 + 2] enone cycloadditions or the asymmetric alkylation of aldehydes, respectively. These papers impacted the field enormously and led to many new synthetic strategies.[9,12−17] This work on transition metal complexes, primarily using iridium and ruthenium, renewed the field of solution-based photocatalysis. However, more recently, organic photocatalysts have become of great interest. Organic photoredox catalysts are generally cheaper to produce and are more sustainable and synthetically tunable than transition metal complexes. In addition, accessing excited state organic radicals can provide reduction potentials that may rival that of alkali metals.[9]

Despite the rapid development and potential of organic photoredox reactions, a comprehensive understanding of the fundamental mechanisms driving these reactions has not kept pace. In fact, recent work[18−20] has called into question the mechanistic role of reactive organic radicals as synthetic intermediates. Mechanism determination has largely been based on indirect methods, e.g., combining redox potential measurements, bond dissociation energies, spectroelectrochemistry, Stern−Volmer measurements, and changes in reagent concentration and type.[21−24] Such measurements can give significant information about individual sections of a reaction but may not provide much information on the critical intermediates.

Received: March 26, 2024
Revised: June 20, 2024
Accepted: July 11, 2024

https://doi.org/10.1021/acs.jpclett.4c00895
J. Phys. Chem. Lett. 2024, 15, 7945−7953

The mechanism of a photoredox reaction using an organic catalyst is generally described in a simplified manner. A closed-shell organic catalyst absorbs light, generating a photoexcited species. Internal conversion may occur from a hot excited state or there may be intersystem crossing to a triplet state. The catalyst can then undergo electron transfer, acting as either an oxidant or reductant depending on the nature of the reaction as shown in Figure 1. Following a charge transfer event, the catalyst

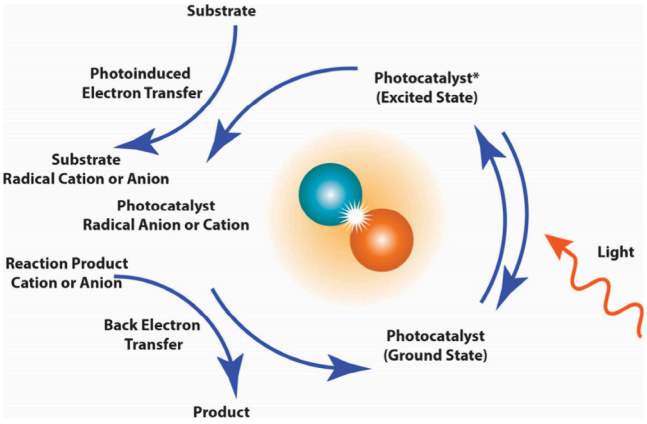

Figure 1. A generalized photoredox catalysis cycle (blue arrows) with a cartoon representing a photoinduced electron transfer event.

is generally reformed with the use of a sacrificial species, usually an amine. There are several issues with this description. It oversimplifies the nature of solution-based photochemistry. For instance, the solvent is not explicitly considered but it can participate in the reaction. This may happen through electrostatic interactions that drive processes like preaggregation or solvent coordination, hydrogen bonding, and even direct participation of the solvent in the reaction. Energy transfer processes may also play a role in the mechanisms of these reactions as well as the physical limits of the process of diffusion. If a photoexcited organic radical is acting as an intermediate species, the lifetime of that species is generally shorter than the time scale of diffusion for a bimolecular reaction in solution. This would imply that additional intermediate processes must occur. This description of an organic photoredox reaction also does not include productive and unproductive reaction pathways. Organic photoredox catalytic reactions often have low yields and require long reaction times with high numbers of turnovers. This suggests that these nonproductive pathways may be significant. In fact, the issue of low "quantum yield" or efficiency has been a major factor in the field.[25] These nonproductive pathways may include the degradation or sequestration of the catalyst, which limits the generation of product. There are many potential pathways to degradation of organic photoredox catalysts including dearomatization reactions[26,27] such as photoinduced Birch reductions or carboxylation. These dearomatization reactions can be highly efficient and significantly limit the number of overall catalytic turnovers. Organic photoredox catalysts can also undergo irreversible breakdown though photodegradation. This can be facilitated by reactions with the solvent or by the formation of complexes with other species in solution. The common use of sacrificial amines in these reactions can also lead to undesirable side reactions that can lead to degradation or transformation of the catalyst. For an individual catalyst, these reactions are expected to occur on a subnanosecond time scale and can be characterized by ultrafast spectroscopy.

The mechanisms of organic photoredox catalytic reactions have generally been rationalized by thermodynamic arguments centered on a determination of ΔG. The change in the Gibbs free energy is estimated from the redox potentials of the excited photocatalyst and the reactant obtained from either electrochemical data or steady-state absorption and fluorescence measurements. The thermodynamic favorability of a photoinduced electron transfer event has been described using the following equation:[28,29]

$$\Delta G = E_{ox}(D^{\bullet+}/D) - E_{red}(A/A^{\bullet-}) - E_{0,0} - \frac{e^2}{4\pi\varepsilon_0\varepsilon r} \quad (1)$$

where $E_{ox}(D^{\bullet+}/D)$ and $E_{red}(A/A^{\bullet-})$ are the ground state oxidation and reduction potentials of the donor and acceptor, respectively. $E_{0,0}$ is the energy of the vibrationally relaxed excited state of the reactant. This is typically estimated in the synthetic organic photoredox catalysis literature as the crossing point between steady-state absorption and fluorescence plots (half the Stokes shift). However, this will only provide a rough estimation as it does not consider other contributions to the absorption and fluorescence line shape. The last term in eq 1 corresponds to the Coulombic stabilization energy associated with the solvent-dependent energy difference induced by charge separation. Equation 1 is sometimes called the Rehm−Weller equation, although this notation is not fully correct[9] as there is another expression also referred to as the Rehm−Weller equation that relates the bimolecular rate constant for photoinduced electron transfer with the change in the Gibbs free energy for that process based on an empirical correlation.[29]

Although eq 1 provides a reasonable starting point for understanding the energy parameters of photoinduced electron transfer in photoredox catalysis, it has limitations. It is a phenomenological expression based on measurements done in the late 1960s.[29,30] These measurements did not account for the existence of the inverted region in the Marcus theory of electron transfer. Instead, they showed that the rate constant of photoinduced electron transfer increased to a diffusion limited value. The existence of the Marcus inversion region has since been demonstrated many times.[31−35] As key steps of photoredox reactions such as those involving benzoquinone and quinolinium catalysts may occur in the Marcus inverted region,[36,37] using Marcus theory directly is more likely to provide an appropriate description of the electron transfer process.[38] In addition, while the use of eq 1 is conceptually straightforward, it disregards kinetic limitations, the specific interactions of the solvent, or that the actual catalytic species might be a transient intermediate. Identifying the processes governing the efficiency and understanding the mechanisms of these photoredox reactions requires direct observation of the steps of the reactions. This can be achieved using time-resolved spectroscopy to track the photocatalyst as it proceeds through the reaction.

There is a long history of time-resolved measurements to study chemical reactions. The 1967 Nobel prize in chemistry was for flash photolysis,[39−41] which has been used extensively to investigate photocatalytic reactions.[42−49] These time-resolved measurements have generally been sensitive to time scales on the order of nanoseconds-to-milliseconds and often use narrow spectral bandwidths. However, generating a measurement to fully map a reaction mechanism requires broadband spectral resolution and time scales from femtoseconds to nanoseconds

https://doi.org/10.1021/acs.jpclett.4c00895
J. Phys. Chem. Lett. 2024, 15, 7945−7953

(and beyond). This photophysical view of a reaction can be used to construct a kinetic scheme and directly observe the intermediates, including both productive and unproductive steps. Mechanistic understanding of these reactions can be used to establish design principles that guide future photocatalyst developments.[50−52] Recent transient absorption (TA) or pump−probe experiments[52−57] have demonstrated the importance of ultrafast spectroscopy to study photoredox catalytic systems. Time-resolved vibrational spectroscopy can also be used to understand the role of specific vibrational modes,[58] vibronic coupling,[59] or charge-transfer reorganization energies[60] on photoredox catalytic processes. Techniques such as two-dimensional infrared spectroscopy,[61] two-dimensional electronic−vibrational spectroscopy,[62] femtosecond stimulated Raman spectroscopy,[63] or visible/ultraviolet pump-infrared probe TA can provide additional information. As demonstrated in the literature,[18,52,54,56,64−71] nonlinear time-resolved spectroscopy can provide powerful insights into the fundamental physical properties driving chemical reactions, allowing for a comprehensive understanding of the underlying mechanisms of organic photoredox catalysis.

The chemical transformations enabled by photoredox catalysis are driven by fundamental photophysical processes. These include energy or charge transfer, proton transfer, vibronic coupling, intersystem crossing, internal conversion, and solvation dynamics among many others as shown in Figure 2. Time-resolved ultrafast methods such as TA or two-dimensional electronic spectroscopy (2DES)[72] can be used to characterized and track these processes, following a photocatalyst as it undergoes the first steps of the chemical reaction. These initial steps are on femto-to-nanosecond time scales and determine the outcome of the catalytic pathway, setting in motion the longer time scale dynamics.

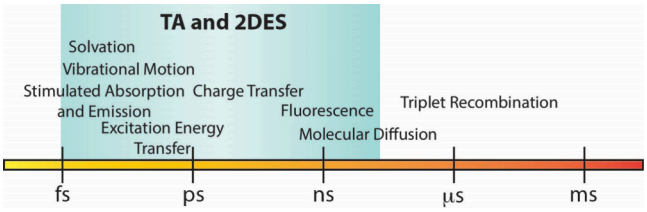

Figure 2. Overview of the time scales of molecular processes in solution associated with photoredox catalysis relative to the time resolution of TA and 2DES. The time resolution of TA and 2DES can extend beyond the nanosecond regime but different delay methods are generally required. The time scale ranges shown here are approximate and longer or shorter time scale outliers exist for all processes shown here.

TA measurements with broadband detection, can follow the evolution of the photocatalyst as it undergoes processes that are central to many proposed photoredox catalytic mechanisms including charge or energy transfer, intersystem crossing, solvation dynamics, and internal conversion.[73,74] The use of broadband laser pulses in TA allows for wide spectral resolution of contributing signals. Generating a map of the excited state evolution for a photocatalyst requires sufficient spectral bandwidth to identify intermediates. These measurements can track the reduction or oxidation of photoredox catalysts and identify any subsequent reactive intermediates. They can distinguish between and follow the evolution of singlet and triplet states. TA can also be used to characterize solvent interactions and help determine the role of solvent in the reaction including the formation of aggregates, preassembled charge transfer complexes, hydrogen bonding, and solvent mediated proton coupled electron transfer, among others. In addition, as TA is an inherently heterodyned measurement, signal contributions can be separated based on their sign.[73] Negative contributions correspond to ground state bleach or stimulated emission. A negative signal in TA corresponds to less absorption, while positive corresponds to more absorption. Ground state bleach represents the depletion of the ground state population due to promotion to the excited state. Fewer molecules available to absorb light resonant with the ground to excited state transition leads to greater transmission and a negative signal. Stimulated emission is generated when a photon from the probe induces emission from the excited molecule, returning it to the ground state. Stimulated emission results in a negative signal as the emission of a photon increases the light that reaches the detector. Positive features are associated with excited state absorption or the generation of photoproduct due to an increase in absorption. Excited state absorption signal appears when transitions to higher or other excited states occur from the excited state of the molecule. This corresponds to an increase in absorption generating a positive signal. Signals associated with photoproducts arise from an increase in absorption and can reveal intermediates or provide other direct information on the mechanism.

Following the dynamics of an organic photoredox catalyst using a time-resolved optical technique such as TA or 2DES imposes requirements on both the maximum delay and experimental time steps. Chemical reactions require molecular collisions or interactions to proceed. At room temperature, the time scale of these interactions is limited by the average time between molecular encounters per the diffusion rate. Estimating a diffusion rate of $\sim 10^9-10^{10}$ M^{-1} s^{-1} and a photocatalyst concentration of 0.1 M gives a limit on molecular interactions on the order of 1−10 ns. Therefore, time delays for the optical experiment must reach the nanosecond regime or beyond. Tracking the dynamics of photoredox catalysts also requires short time-resolution to capture processes such as internal conversion on <100 fs time scales and energy transfer on picosecond time scales. Intermediate radical species may only have picosecond lifetimes and we expect solvent reorganization and other related effects to occur in femtoseconds to picoseconds. Triplet relaxation may occur beyond a μs time scale. These requirements equate to an apparatus capable of long time-delays and high-resolution short time-delays simultaneously. This simultaneous detection over many decades of time can allow for the correlation of charge or energy transfer with generation of product and triplet recombination. However, there are practical limitations to building a single time-resolved measurement connecting time scales from fs to μs (or even beyond). Short time delays are often achieved by optical gating, interference, or physical delays. These approaches are not effective for long time delays as interference fringes become too close together or physical delays become unreasonably long. Longer time delays are often accomplished using electronics. These two approaches to time delays are generally incompatible, making it difficult to construct a single instrument. Currently, apparatuses that can achieve a wide range of time scales have been built using two different pathlengths for time delays with a shorter distance for fs to ps and a longer one for up to tens of ns.

While TA provides an overall survey of the dynamics of the excited states, 2DES can allow for greater resolution and selectivity. 2DES has been primarily used to measure energy

https://doi.org/10.1021/acs.jpclett.4c00895
J. Phys. Chem. Lett. 2024, 15, 7945−7953

transfer and vibrational coupling, which is not the focus of its application to photoredox catalysis. Instead, it can be used to get a greater understanding of spectral line shape, which can identify overlapped intermediates, and to provide an extra dimension that can allow for separation of components that may be hidden in TA measurements.

Figure 3 shows data collected on a Cu(II)−tripyrrindione neutral radical complex.[75−77] These complexes are redox-active,

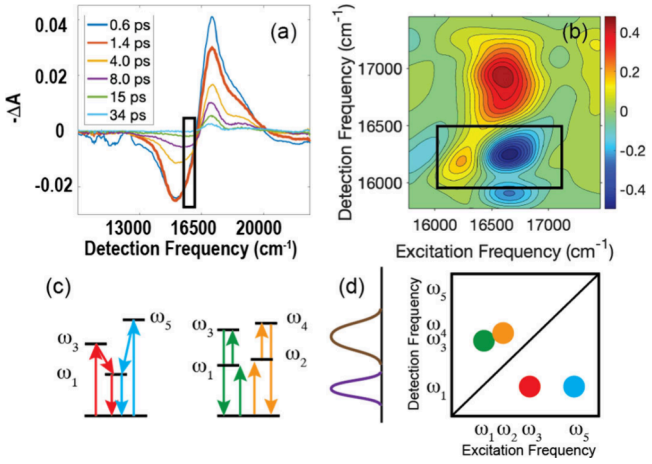

Figure 3. Data for a Cu(II)−tripyrrindione complex at room temperature. The boxed region is the same in both (a) and (b). Panel (a) shows TA data and (b) shows 2DES data (1.4 ps pump−probe delay time). The 1.4 ps pump−probe delay time TA trace in (a) is thicker to highlight the comparison to the 2DES plot. In the 2DES plot, there is a positive feature at 16200 cm^{-1} emission (black box), which is hidden in (b) because of the integration over the excitation axis. The black boxes in panel (a) and (b) correspond to the same regions. Panels (c) and (d) are representations of energy or charge transfer signal contributions relevant to photoredox catalysis. (c) Signal contributions for the peaks in the cartoon 2DES and TA in panel (d). The colors in (c) correspond to the peaks in (d). The left side of (d) shows the corresponding TA plot, where much of the detail is lost. The colors in the TA cartoon are representative of the mixing of signal contributions.

reversibly perform one electron oxidation and reduction and are candidate photoredox catalysts. The boxes in (a) and (b) indicate the same regions in both data sets, where the TA signal is negative while the 2DES shows negative and positive signal components. Since the sign of the signal is reversed between 2DES and TA (a positive signal in TA is negative in 2DES and vice versa), a direct comparison can be made by multiplying the TA data by −1. This has been done for the data presented in Figure 3a and is represented by the *y*-axis label of $-\Delta A$. The positive component, associated with stimulated emission, is hidden in the TA measurements. To aid comparison, the TA signal corresponds to a summation over the horizontal axis of the 2DES measurement. In this case, the larger negative signal obscures the smaller positive component. While both signal components are in the TA data, it is difficult to separate out the positive signal at 16200 cm^{-1}. In complex photocatalytic reaction mixtures with multiple pathways and intermediates, additional information from 2DES may assist in identifying overlapping contributions to the signal. For example, more than one charge-transfer process may produce a signal at the same or similar energy. In a TA measurement, these would overlap, whereas in 2DES the signal contributions can be spatially separated. Figure 3a,b show an example of signals that are separable in 2DES and hidden in TA. The positive and negative signal contributions shown in the box in Figure 3b are resolved in the 2DES measurement. However, in TA these are summed over each other, resulting in a cancelation of signals. This leaves only a negative signal as shown in the box in Figure 3a. While the two signal components are clear in the 2DES measurement, it would be difficult to identify that there was a positive signal hidden under the larger negative signal in the TA data. Figure 3c,d present a cartoon representation of possible electron transfer or other processes related to photoredox catalysis that could lead to signal cancelation and how they might appear in TA and 2DES. The red and blue pathways shown in Figure 3c represent two different excited states that relax through a state or states at similar energy. Signals associated with electron transfer events may follow a similar path. The green and orange pathways represent an excited state absorption or a photoproduct generation, which is common in photoredox catalysis. Figure 3d shows how the pathways in panel (c) would appear as separate signal contributions on a 2DES plot and as single features in TA (plot on the left side of panel (d)).

The field of organic photoredox catalysis has many open questions. These include a disparity between the lifetime of organic radicals and diffusion limits for bimolecular reactions, the specifics of early/intermediate steps that determine the trajectories of light-activated catalytic reactions, the identity of

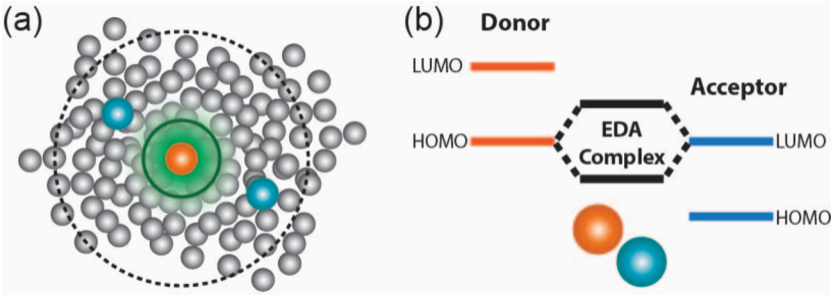

Figure 4. (a) Cartoon schematic representing diffusion limits and excited state lifetimes for photoredox catalysis. The gray, blue, and orange spheres are solvent molecules, reactants, and the photocatalyst, respectively. The green circle represents the diffusion limit of a photoexcited organic radical. Since the lifetime of an organic radical is expected to be short, the photocatalyst may not diffuse far enough, on average, to encounter a reactant molecule. The black dashed line circle represents the photoexcited diffusion limit of a longer-lived closed shell species. The longer lifetime of the closed-shell species results in a longer diffusion limit while the photocatalyst is in the excited state, increasing the likelihood of encountering a reactant. (b) Molecular orbital representation of the formation of an electron donor−acceptor (EDA) complex with a cartoon representation of the association between donor and acceptor molecules.

https://doi.org/10.1021/acs.jpclett.4c00895
J. Phys. Chem. Lett. 2024, 15, 7945−7953

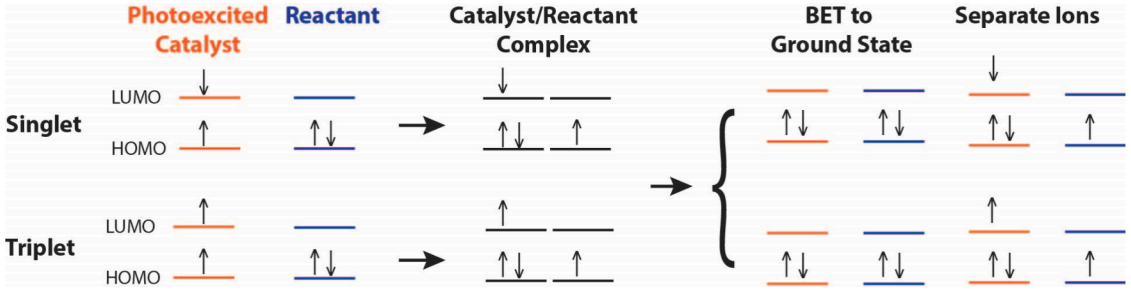

Figure 5. Molecular orbital representation of an electron transfer process where the catalyst is reduced (reductive quenching). The organic photocatalyst is excited to a singlet or triplet state while the reactant or substrate is in the ground state. Once the photoexcited catalyst encounters the reactant, charge transfer can occur. The contact ion pair has the same spin as the photoexcited catalyst. Following charge transfer, both molecules can end up in the ground state via back electron transfer (BET) or as separate ions. Since BET from the triplet requires intersystem crossing, it is expected to be slower.

transient intermediate species, productive versus unproductive pathways, and the potential role of solvent as a critical intermediary.

Organic photoredox catalysts have been used in reactions that require reduction potentials comparable to alkali metals[78,79] by accessing the excited state of the radical species. However, organic radicals tend to be short-lived. The excited-state lifetimes of many organic radical species are generally considered to be too short (picoseconds) to be the key drivers of photoredox catalytic reactions due to temporal limits on binuclear reactions (nanoseconds). If the diffusion limited average time scale for the photoexcited catalyst to encounter a reactant is longer than the lifetime of the excited state, then the probability that a reaction will occur is low. The reaction would only proceed if the reactant happened to be close to the photocatalyst immediately following photoexcitation. This is represented in Figure 4a. If excited-state reactive open-shell doublet radicals do not participate directly in the electron transfer steps of photoredox catalysis due to their short lifetimes, then many proposed mechanisms may be incomplete and missing reactive intermediates. However, reactions requiring high reduction potentials have been observed using organic photoredox catalysts.[18,78−80] Possible explanations for the action of these photocatalysts include preaggregation or other physical association between catalyst and substrate to circumvent diffusion limits. For example, studies on the catalytic activity of 9,10-dicyanoanthracene radical anion[81] suggest that it is enabled by preaggregation. Another possible explanation involves the conversion of the open-shell radical to a closed-shell species that then participates in the reaction, or the direct participation of solvent through reduction or oxidation processes. The Nocera group[18] used TA measurements to show that a Meisenheimer complex of naphthalene monoimide was the catalytic species rather than the corresponding radical anion. Subsequent work on benzo[ghi]perylene monoimides[82] has also shown that reactions can be enabled by reactive intermediates rather than a short-lived organic radical.

The short lifetimes and optical characteristics of organic radicals also affects standard optical characterization methods that involve steady-state absorption and fluorescence. In steady-state absorption, the lowest lying electronic transition of a radical species is usually a doublet state, D_1. This state generally has low oscillator strength.[83] Stronger absorption features in the visible that could be targeted for photoredox catalysis are higher lying doublet states. In addition, organic radicals tend to not have significant fluorescence. This is due to their short excited-state lifetimes as well as the presence of low-lying states with small oscillator strength in agreement with energy gap law.[84] These factors make estimation of the thermodynamic driving force for the photoinduced electron transfer challenging using an expression such as eq 1.

The role of the solvent in the mechanisms of photoredox catalysis represents another open question in the field. While it is well-known that the dielectric constant of the solvent influences the rate of charge transfer events, and therefore the efficiency of the reaction, more direct involvement has not been thoroughly investigated. With sufficiently high reduction or oxidation potentials, the solvent may act as an electron donor or acceptor. Solvent reduction by the excited state of an organic radical may also generate a longer lived intermediate that can allow the reaction to proceed. Studies on a system with an amide solvent[85] showed that it participated in the catalytic mechanism while many photoredox arylation reactions[86] are also enabled by direct involvement of the solvent.

Solvents are known to participate in photoinduced processes in solution. They can promote nonradiative transitions, hydrogen-bond or participate in proton and charge transfer events. Solvents may coordinate to photocatalysts or reactants, potentially modifying the rate of reactions. Coordination could support the formation of ground state electron donor−acceptor (EDA) complexes or charge transfer complexes that are known to be part of the mechanism of certain photoredox catalysis reactions.[9,87−89] The basic level structure of an EDA complex is shown in Figure 4b. In contrast to ground state EDA complexes, exciplexes are formed in the excited state generally between an electron poor catalyst and electron rich substrate.[9] Exciplexes may play a similar role to EDA complexes in circumventing issues with diffusion limits. A systematic investigation of the role of the solvent in photoredox catalysis mechanisms using time-resolved spectroscopy may lead to new methods to control the selectivity of reactions and improve their efficiency.

In addition to highly reducing or oxidizing radical species, many closed-shell molecules act as photoredox catalysts and participate as intermediates in photocatalytic reactions. Organic closed-shell species generally have longer lived excited states as compared to organic radicals. This potentially avoids the diffusion limit issue that may hamper the action of the excited state of organic radicals as photocatalysts. Singlet states tend to be higher in energy than triplet states and, as such, singlet states are usually stronger reductants or oxidants. In comparison, the longer lifetime of triplet states due to intersystem crossing allows for a longer diffusion time for bimolecular interactions and electron transfer events to occur. Triplet states may be favorable for another reason that has not been widely investigated:

https://doi.org/10.1021/acs.jpclett.4c00895
J. Phys. Chem. Lett. 2024, 15, 7945−7953

reduced probability of back electron transfer. If we consider a reductive quenching process, the contact ion pair that is formed as a part of the electron transfer event between the photocatalyst and the reactant should have the same spin multiplicity as the photocatalyst as shown in Figure 5. For a triplet state, back electron transfer would require intersystem crossing and would be slower than back electron transfer involving a singlet state.[9] Back electron transfer processes compete with the desired catalytic reaction, reducing the overall efficiency. Minimizing this issue by favoring triplet states may result in higher product yields. Time-resolved spectroscopy can be used to identify the time scales associated with photoredox reactions driven by triplet states, compare these to related singlet states processes and determine the back electron transfer rates to evaluate the effect of triplet states on the efficiency of the reaction.

The role of triplet states in photoredox catalysis can be modified with the use of sensitizers or quenchers. Triplet sensitizers facilitate triplet associated pathways while quenchers generally open alternative relaxation mechanisms that reduce the involvement of triplet states. Quenchers can be added to reactions thought to proceed via a triplet state to validate their involvement in the reaction mechanism by blocking those pathways or they can be used to reduce unproductive side reactions. Common classes of triplet sensitizers used in photoredox catalysis include xanthones, xanthenes, and flavins.[90] Sensitizers such as an Ir(III) isocyanoborato molecule along with other transition metal complexes have been used for triplet−triplet energy transfer catalysis,[91] butane-2,3-dione and 2,5-diphenyloxazole for triplet upconversion,[92] BODIPY dyes[93] and phenothiazines[94] as triplet sensitizers, methylene blue with a triplet quantum yield of over 0.5 has been used for oxidative hydroxylation reactions,[22,95] among many others. As oxygen is a well-known triplet quencher,[22,96] triplet-state involved mechanisms can be identified by comparing experiments performed in the absence and the presence of oxygen. Other molecules such as vicinal dibromide[22] or (2,2,6,6-tetramethylpiperidin-1-yl)-oxidanyl (TEMPO)[97] can also act as efficient triplet quenchers.

In spectroscopy, the term quantum yield often refers to the ratio of photons emitted as fluorescence relative to the number of photons absorbed by a molecule. In the field of photoredox catalysis, quantum yield instead represents the units of product generated per photon absorbed by the photocatalyst. Although it is a powerful approach to chemical synthesis, photoredox catalysis tends to have low quantum yields.[25] Low quantum yield (low efficiency) reactions require more intense light sources being used for longer times, often 24−48 h, to generate a reasonable amount of product. This had led to significant issues with scaling up reactions for industrial and pharmaceutical applications. High photocatalyst loadings are used to offset the lower efficiency but this causes issues with light absorption in reactors. A higher concentration of light absorbing photocatalyst results in greater opacity of the solution and shallower depth penetration of the light, lowering the yield. In addition, organic photocatalysts that absorb visible light have relatively planar conjugated structures. While this allows for longer wavelength absorption, it can also mean that these molecules are likely to pi-stack or aggregate. As a result, increasing the concentration may lead to more photocatalyst sequestered in aggregates not participating in the reaction mechanism and lowering the yield.[95] Strategies for increasing efficiency per photon are important to the long-term growth and stability of the field. As the photoredox quantum yield is defined in terms of efficiency per input photons, time-resolved optical spectroscopy methods are particularly well suited to addressing this issue.

The consideration of the feasibility of organic photoredox reactions has been primarily focused on thermodynamic considerations and the presence of accessible visible absorption features associated with the photocatalyst. This approach largely disregards kinetics, pathways involving multiple intermediates, and other considerations such as direct solvent involvement or molecular interactions. A new approach to understanding organic photoredox catalytic reactions is needed. Time-resolved spectroscopic optical techniques can reveal the mechanisms and intermediate states that enable photoredox catalytic processes under reaction conditions. Through these techniques, it is possible to identify the driving forces and the intermediate states for photoredox catalytic reactions, which will open pathways for the design of new, more efficient catalysts.

AUTHOR INFORMATION

Corresponding Author

Vanessa M. Huxter − *Department of Chemistry and Biochemistry and Department of Physics, University of Arizona, Tucson, Arizona 85721, United States;* orcid.org/0000-0001-9692-5312; Email: vhuxter@arizona.edu

Complete contact information is available at: https://pubs.acs.org/10.1021/acs.jpclett.4c00895

Notes

The author declares no competing financial interest.

ACKNOWLEDGMENTS

V.M.H. gratefully acknowledges support from the donors of the American Chemical Society Petroleum Research Fund through Grant 65536-ND6 and support from the National Science Foundation through a CAREER Award (Grant 2236610). V.M.H. thanks Dr. Elisa Tomat and Dr. Ritika Gautam for providing the Cu(II)−tripyrrindione sample and Dr. Byungmoon Cho and Dr. Alicia Swain for the TA and 2DES measurements on the Cu(II)−tripyrrindione.

REFERENCES

(1) Shaw, M. H.; Twilton, J.; MacMillan, D. W. C. Photoredox catalysis in organic chemistry. *J. Org. Chem.* **2016**, *81* (16), 6898−6926.
(2) McAtee, R. C.; McClain, E. J.; Stephenson, C. R. J. Illuminating photoredox catalysis. *Trends in Chemistry* **2019**, *1* (1), 111−125.
(3) Nicholls, T. P.; Leonori, D.; Bissember, A. C. Applications of visible light photoredox catalysis to the synthesis of natural products and related compounds. *Nat. Prod. Rep.* **2016**, *33* (11), 1248−1254.
(4) Douglas, J. J.; Sevrin, M. J.; Stephenson, C. R. J. Visible light photocatalysis: applications and new disconnections in the synthesis of pharmaceutical agents. *Org. Process Res. Dev.* **2016**, *20* (7), 1134−1147.
(5) Sheldon, R. A. Metrics of green chemistry and sustainability: past, present, and future. *ACS Sustain. Chem. Eng.* **2018**, *6* (1), 32−48.
(6) Crisenza, G. E. M.; Melchiorre, P. Chemistry glows green with photoredox catalysis. *Nat. Commun.* **2020**, *11* (1), 803.
(7) Eibner, A. Action of light on pigments I. *Chem. ZTG* **1911**, *35*, 753−755.
(8) Hedstrand, D. M.; Kruizinga, W. H.; Kellogg, R. M. Light induced and dye accelerated reductions of phenacyl onium salts by 1,4-dihydropyridines. *Tetrahedron Lett.* **1978**, *19*, 1255−1258.
(9) Romero, N. A.; Nicewicz, D. A. Organic photoredox catalysis. *Chem. Rev.* **2016**, *116* (17), 10075−10166.
(10) Ischay, M. A.; Anzovino, M. E.; Du, J.; Yoon, T. P. Efficient visible light photocatalysis of [2 + 2] enone cycloadditions. *J. Am. Chem. Soc.* **2008**, *130* (39), 12886−12887.

(11) Nicewicz, D. A.; MacMillan, D. W. C. Merging photoredox catalysis with organocatalysis: the direct asymmetric alkylation of aldehydes. *Science* **2008**, *322* (5898), 77−80.
(12) Narayanam, J. M. R.; Stephenson, C. R. J. Visible light photoredox catalysis: applications in organic synthesis. *Chem. Soc. Rev.* **2011**, *40* (1), 102−113.
(13) Prier, C. K.; Rankic, D. A.; MacMillan, D. W. C. Visible light photoredox catalysis with transition metal complexes: applications in organic synthesis. *Chem. Rev.* **2013**, *113* (7), 5322−5363.
(14) Yoon, T. P. Photochemical stereocontrol using tandem photoredox−chiral lewis acid catalysis. *Acc. Chem. Res.* **2016**, *49* (10), 2307−2315.
(15) Matsui, J. K.; Lang, S. B.; Heitz, D. R.; Molander, G. A. Photoredox-mediated routes to radicals: the value of catalytic radical generation in synthetic methods development. *ACS Catal.* **2017**, *7* (4), 2563−2575.
(16) Nagib, D. A.; MacMillan, D. W. C. Trifluoromethylation of arenes and heteroarenes by means of photoredox catalysis. *Nature* **2011**, *480* (7376), 224−228.
(17) Shi, L.; Xia, W. Photoredox functionalization of C−H bonds adjacent to a nitrogen atom. *Chem. Soc. Rev.* **2012**, *41* (23), 7687−7697.
(18) Rieth, A. J.; Gonzalez, M. I.; Kudisch, B.; Nava, M.; Nocera, D. G. How radical are "radical" photocatalysts? A closed-shell meisenheimer complex is identified as a super-reducing photoreagent. *J. Am. Chem. Soc.* **2021**, *143* (35), 14352−14359.
(19) Mena, L. D.; Borioni, J. L.; Caby, S.; Enders, P.; Argüello Cordero, M. A.; Fennel, F.; Francke, R.; Lochbrunner, S.; Bardagi, J. I. Quantitative prediction of excited-state decay rates for radical anion photocatalysts. *Chem. Commun.* **2023**, *59* (64), 9726−9729.
(20) Sun, R.; Liu, M.; Wang, P.; Qin, Y.; Schnedermann, C.; Maher, A. G.; Zheng, S.-L.; Liu, S.; Chen, B.; Zhang, S.; et al. Syntheses and properties of metalated tetradehydrocorrins. *Inorg. Chem.* **2022**, *61* (31), 12308−12317.
(21) Arias-Rotondo, D. M.; McCusker, J. K. The photophysics of photoredox catalysis: A roadmap for catalyst design. *Chem. Soc. Rev.* **2016**, *45* (21), 5803−5820.
(22) Pitre, S. P.; McTiernan, C. D.; Scaiano, J. C. Understanding the kinetics and spectroscopy of photoredox catalysis and transition-metal-free alternatives. *Acc. Chem. Res.* **2016**, *49* (6), 1320−1330.
(23) Blanksby, S. J.; Ellison, G. B. Bond dissociation energies of organic molecules. *Acc. Chem. Res.* **2003**, *36* (4), 255−263.
(24) Waidmann, C. R.; Miller, A. J. M.; Ng, C.-W. A.; Scheuermann, M. L.; Porter, T. R.; Tronic, T. A.; Mayer, J. M. Using combinations of oxidants and bases as PCET reactants: thermochemical and practical considerations. *Energy Environ. Sci.* **2012**, *5* (7), 7771−7780.
(25) Swierk, J. R. The cost of quantum yield. *Org. Process Res. Dev.* **2023**, *27* (7), 1411−1419.
(26) Kron, K. J.; Rodriguez-Katakura, A.; Elhessen, R.; Mallikarjun Sharada, S. Photoredox chemistry with organic catalysts: role of computational methods. *ACS Omega* **2021**, *6* (49), 33253−33264.
(27) Barltrop, J. A. The photoreduction of aromatic systems. *Pure Appl. Chem.* **1973**, *33* (2−3), 179−196.
(28) Vauthey, E. Elucidating the mechanism of bimolecular photoinduced electron transfer reactions. *J. Phys. Chem. B* **2022**, *126* (4), 778−788.
(29) Rehm, D.; Weller, A. Kinetics of fluorescence quenching by electron and H-atom transfer. *Isr. J. Chem.* **1970**, *8* (2), 259−271.
(30) Rehm, D.; Weller, A. Kinetics and mechanics of electron transfer during fluorescence quenching in acetonitrile. *Ber. Bunsenges.* **1969**, *73*, 834.
(31) Miller, J. R.; Calcaterra, L. T.; Closs, G. L. Intramolecular long-distance electron transfer in radical anions: the effects of free energy and solvent on the reaction rates. *J. Am. Chem. Soc.* **1984**, *106* (10), 3047−3049.
(32) Closs, G. L.; Miller, J. R. Intramolecular Long-Distance Electron Transfer in Organic Molecules. *Science* **1988**, *240* (4851), 440−447.
(33) Wasielewski, M. R.; Niemczyk, M. P.; Svec, W. A.; Pewitt, E. B. Dependence of rate constants for photoinduced charge separation and dark charge recombination on the free energy of reaction in restricted-distance porphyrin-quinone molecules. *J. Am. Chem. Soc.* **1985**, *107* (4), 1080−1082.
(34) Guldi, D. M.; Asmus, K.-D. Electron transfer from C76 (C'_{2v}) and C78 (D_2) to radical cations of various arenes: evidence for the Marcus inverted region. *J. Am. Chem. Soc.* **1997**, *119* (24), 5744−5745.
(35) Smitha, M. A.; Prasad, E.; Gopidas, K. R. Photoinduced electron transfer in hydrogen bonded donor−acceptor systems: free energy and distance dependence studies and an analysis of the role of diffusion. *J. Am. Chem. Soc.* **2001**, *123* (6), 1159−1165.
(36) Gould, I. R.; Ege, D.; Moser, J. E.; Farid, S. Efficiencies of photoinduced electron-transfer reactions: role of the Marcus inverted region in return electron transfer within geminate radical-ion pairs. *J. Am. Chem. Soc.* **1990**, *112* (11), 4290−4301.
(37) Gould, I. R.; Moser, J. E.; Armitage, B.; Farid, S.; Goodman, J. L.; Herman, M. S. Electron-transfer reactions in the Marcus inverted region. Charge recombination versus charge shift reactions. *J. Am. Chem. Soc.* **1989**, *111* (5), 1917−1919.
(38) Rosspeintner, A.; Angulo, G.; Vauthey, E. Bimolecular photoinduced electron transfer beyond the diffusion limit: the Rehm−Weller experiment revisited with femtosecond time resolution. *J. Am. Chem. Soc.* **2014**, *136* (5), 2026−2032.
(39) Porter, G. The absorption spectroscopy of substances of short life. *Disc. Faraday Soc.* **1950**, *9*, 60−69.
(40) Eigen, M. Methods for investigation of ionic reactions in aqueous solutions with half-times as short as 10^{-9} s. Application to neutralization and hydrolysis reactions. *Disc. Faraday Soc.* **1954**, *17* (0), 194−205.
(41) Norrish, R. G. W. Free radicals in explosions studied by flash photolysis. *Disc. Faraday Soc.* **1953**, *14* (0), 16−22.
(42) Kamat, P. V.; Fox, M. A. Photosensitization of TiO_2 colloids by erythrosin b in acetonitrile. *Chem. Phys. Lett.* **1983**, *102* (4), 379−384.
(43) Ryan, M. A.; Fitzgerald, E. C.; Spitler, M. T. Internal reflection flash photolysis study of the photochemistry of eosin at titania semiconductor electrodes. *J. Phys. Chem.* **1989**, *93* (16), 6150−6156.
(44) Arbour, C.; Sharma, D. K.; Langford, C. H. Picosecond flash spectroscopy of titania colloids with adsorbed dyes. *J. Phys. Chem.* **1990**, *94* (1), 331−335.
(45) Kamat, P. V. Picosecond charge-transfer events in the photosensitization of colloidal titania. *Langmuir* **1990**, *6* (2), 512−513.
(46) Frei, H.; Fitzmaurice, D. J.; Graetzel, M. Surface chelation of semiconductors and interfacial electron transfer. *Langmuir* **1990**, *6* (1), 198−206.
(47) Romero, N. A.; Nicewicz, D. A. Mechanistic insight into the photoredox catalysis of anti-markovnikov alkene hydrofunctionalization reactions. *J. Am. Chem. Soc.* **2014**, *136* (49), 17024−17035.
(48) Pitre, S. P.; McTiernan, C. D.; Ismaili, H.; Scaiano, J. C. Mechanistic insights and kinetic analysis for the oxidative hydroxylation of arylboronic acids by visible light photoredox catalysis: A metal-free alternative. *J. Am. Chem. Soc.* **2013**, *135* (36), 13286−13289.
(49) Pitre, S. P.; McTiernan, C. D.; Ismaili, H.; Scaiano, J. C. Metal-free photocatalytic radical trifluoromethylation utilizing methylene blue and visible light irradiation. *ACS Catal.* **2014**, *4* (8), 2530−2535.
(50) Ruccolo, S.; Qin, Y.; Schnedermann, C.; Nocera, D. G. General strategy for improving the quantum efficiency of photoredox hydroamidation catalysis. *J. Am. Chem. Soc.* **2018**, *140* (44), 14926−14937.
(51) Thompson, W. A.; Sanchez Fernandez, E.; Maroto-Valer, M. M. Review and analysis of CO_2 photoreduction kinetics. *ACS Sustain. Chem. Eng.* **2020**, *8* (12), 4677−4692.
(52) Orr-Ewing, A. J. Perspective: How can ultrafast laser spectroscopy inform the design of new organic photoredox catalysts for chemical and materials synthesis? *Struct. Dyn.* **2019**, *6* (1), No. 010901.
(53) Müller, C.; Isakov, D.; Rau, S.; Dietzek, B. Influence of the protonation state on the excited-state dynamics of ruthenium(II) complexes with imidazole π-extended dipyridophenazine ligands. *J. Phys. Chem. A* **2021**, *125* (27), 5911−5921.
(54) Stevenson, B. G.; Spielvogel, E. H.; Loiaconi, E. A.; Wambua, V. M.; Nakhamiyayev, R. V.; Swierk, J. R. Mechanistic investigations of an α-aminoarylation photoredox reaction. *J. Am. Chem. Soc.* **2021**, *143* (23), 8878−8885.

https://doi.org/10.1021/acs.jpclett.4c00895
J. Phys. Chem. Lett. 2024, 15, 7945−7953

(55) Lauenstein, R.; Mader, S. L.; Derondeau, H.; Esezobor, O. Z.; Block, M.; Römer, A. J.; Jandl, C.; Riedle, E.; Kaila, V. R. I.; Hauer, J.; et al. The central role of the metal ion for photoactivity: Zn− vs. Ni−Mabiq. *Chem. Sci.* **2021**, *12* (21), 7521−7532.
(56) Bhattacherjee, A.; Sneha, M.; Lewis-Borrell, L.; Amoruso, G.; Oliver, T. A. A.; Tyler, J.; Clark, I. P.; Orr-Ewing, A. J. Singlet and triplet contributions to the excited-state activities of dihydrophenazine, phenoxazine, and phenothiazine organocatalysts used in atom transfer radical polymerization. *J. Am. Chem. Soc.* **2021**, *143* (9), 3613−3627.
(57) Shields, B. J.; Kudisch, B.; Scholes, G. D.; Doyle, A. G. Long-lived charge-transfer states of nickel(II) aryl halide complexes facilitate bimolecular photoinduced electron transfer. *J. Am. Chem. Soc.* **2018**, *140* (8), 3035−3039.
(58) Bredenbeck, J.; Helbing, J.; Hamm, P. Labeling vibrations by light: ultrafast transient 2D-IR spectroscopy tracks vibrational modes during photoinduced charge transfer. *J. Am. Chem. Soc.* **2004**, *126* (4), 990−991.
(59) Hestand, N. J.; Spano, F. C. Expanded theory of H- and J-molecular aggregates: the effects of vibronic coupling and intermolecular charge transfer. *Chem. Rev.* **2018**, *118* (15), 7069−7163.
(60) Myers, A. B. Resonance Raman intensities and charge-transfer reorganization energies. *Chem. Rev.* **1996**, *96* (3), 911−926.
(61) Park, S.; Kwak, K.; Fayer, M. D. Ultrafast 2D-IR vibrational echo spectroscopy: a probe of molecular dynamics. *Laser Phys. Lett.* **2007**, *4* (10), 704.
(62) Dong, H.; Lewis, N. H. C.; Oliver, T. A. A.; Fleming, G. R. Determining the static electronic and vibrational energy correlations via two-dimensional electronic-vibrational spectroscopy. *J. Chem. Phys.* **2015**, *142* (17), 174201.
(63) Kukura, P.; McCamant, D. W.; Mathies, R. A. Femtosecond stimulated Raman spectroscopy. *Annu. Rev. Phys. Chem.* **2007**, *58*, 461−488.
(64) Sneha, M.; Thornton, G. L.; Lewis-Borrell, L.; Ryder, A. S. H.; Espley, S. G.; Clark, I. P.; Cresswell, A. J.; Grayson, M. N.; Orr-Ewing, A. J. Photoredox-HAT catalysis for primary amine α-C−H alkylation: mechanistic insight with transient absorption spectroscopy. *ACS Catal.* **2023**, *13* (12), 8004−8013.
(65) Whitaker, W.; Sazanovich, I. V.; Kwon, Y.; Jeon, W.; Kwon, M. S.; Orr-Ewing, A. J. Characterization of the reversible intersystem crossing dynamics of organic photocatalysts using transient absorption spectroscopy and time-resolved fluorescence spectroscopy. *J. Phys. Chem. A* **2023**, *127* (51), 10775−10788.
(66) Datta, P.; Goswami, T.; Kandoth, N.; Banik, A.; Ahmed, J.; Bhaskaran, A. S.; Saha, R.; Kuniyil, R.; Ghosh, H. N.; Mandal, S. K. Generation of photoinduced phenalenyl-based radicals: towards designing reductive C−C coupling catalysis. *ChemPhotoChem.* **2023**, *7* (6), No. e202300033.
(67) Jeong, D. Y.; Lee, D. S.; Lee, H. L.; Nah, S.; Lee, J. Y.; Cho, E. J.; You, Y. Evidence and governing factors of the radical-ion photoredox catalysis. *ACS Catal.* **2022**, *12* (10), 6047−6059.
(68) Sneha, M.; Bhattacherjee, A.; Lewis-Borrell, L.; Clark, I. P.; Orr-Ewing, A. J. Structure-dependent electron transfer rates for dihydrophenazine, phenoxazine, and phenothiazine photoredox catalysts employed in atom transfer radical polymerization. *J. Phys. Chem. B* **2021**, *125* (28), 7840−7854.
(69) Thornton, G. L.; Phelps, R.; Orr-Ewing, A. J. Transient absorption spectroscopy of the electron transfer step in the photochemically activated polymerizations of N-ethylcarbazole and 9-phenylcarbazole. *Phys. Chem. Chem. Phys.* **2021**, *23* (34), 18378−18392.
(70) Iwata, K. Ultrafast bimolecular radical reaction between S1p-terphenyl and carbon tetrachloride: mode-specific acceleration of vibrational dephasing in reactant molecule. *J. Raman Spectrosc.* **2008**, *39* (11), 1512−1517.
(71) Martin, M. M.; Plaza, P.; Changenet-Barret, P.; Siemiarczuk, A. UV−vis subpicosecond spectroscopy of 4-(9-Anthryl)-N,N′-dimethylaniline in polar and nonpolar solvents: a two-dimensional view of the photodynamics. *J. Phys. Chem. A* **2002**, *106* (10), 2351−2358.
(72) Maiuri, M.; Garavelli, M.; Cerullo, G. Ultrafast spectroscopy: state of the art and open challenges. *J. Am. Chem. Soc.* **2020**, *142* (1), 3−15.
(73) Berera, R.; van Grondelle, R.; Kennis, J. T. M. Ultrafast transient absorption spectroscopy: principles and application to photosynthetic systems. *Photosynth. Res.* **2009**, *101* (2−3), 105−118.
(74) Ruckebusch, C.; Sliwa, M.; Pernot, P.; de Juan, A.; Tauler, R. Comprehensive data analysis of femtosecond transient absorption spectra: A review. *J. Photochem. Photobiol. C* **2012**, *13* (1), 1−27.
(75) Cho, B.; Swain, A.; Gautam, R.; Tomat, E.; Huxter, V. M. Time-resolved dynamics of stable open- and closed-shell neutral radical and oxidized tripyrrindione complexes. *Phys. Chem. Chem. Phys.* **2022**, *24* (26), 15718−15725.
(76) Kumar, A.; Thompson, B.; Gautam, R.; Tomat, E.; Huxter, V. Temperature-dependent spin-driven dimerization determines the ultrafast dynamics of a copper(II)-bound tripyrrindione radical. *J. Phys. Chem. Lett.* **2023**, *14* (50), 11268−11273.
(77) Gautam, R.; Astashkin, A. V.; Chang, T. M.; Shearer, J.; Tomat, E. Interactions of metal-based and ligand-based electronic spins in neutral tripyrrindione π dimers. *Inorg. Chem.* **2017**, *56* (11), 6755−6762.
(78) MacKenzie, I. A.; Wang, L. F.; Onuska, N. P. R.; Williams, O. F.; Begam, K.; Moran, A. M.; Dunietz, B. D.; Nicewicz, D. A. Discovery and characterization of an acridine radical photoreductant. *Nature* **2020**, *580* (7801), 76−80.
(79) Cowper, N. G. W.; Chernowsky, C. P.; Williams, O. P.; Wickens, Z. K. Potent reductants via electron-primed photoredox catalysis: unlocking aryl chlorides for radical coupling. *J. Am. Chem. Soc.* **2020**, *142* (5), 2093−2099.
(80) Cole, J. P.; Chen, D.-F.; Kudisch, M.; Pearson, R. M.; Lim, C.-H.; Miyake, G. M. Organocatalyzed birch reduction driven by visible light. *J. Am. Chem. Soc.* **2020**, *142* (31), 13573−13581.
(81) Glaser, F.; Wenger, O. S. Red light-based dual photoredox strategy resembling the Z-scheme of natural photosynthesis. *JACS Au* **2022**, *2* (6), 1488−1503.
(82) Sau, A.; Pompetti, N. F.; Green, A. R.; Popescu, M. V.; Paton, R. S.; Miyake, G. M.; Damrauer, N. H. Mechanistic investigation of a photocatalyst model reveals function by perylene-like closed shell super-photoreductant capable of reducing unactivated arenes. *ACS Catal.* **2024**, *14* (4), 2252−2263.
(83) Abdurahman, A.; Hele, T. J. H.; Gu, Q.; Zhang, J.; Peng, Q.; Zhang, M.; Friend, R. H.; Li, F.; Evans, E. W. Understanding the luminescent nature of organic radicals for efficient doublet emitters and pure-red light-emitting diodes. *Nat. Mater.* **2020**, *19* (11), 1224−1229.
(84) Englman, R.; Jortner, J. The energy gap law for radiationless transitions in large molecules. *Mol. Phys.* **1970**, *18* (2), 145−164.
(85) Toriumi, N.; Yamashita, K.; Iwasawa, N. Metal-free photoredox-catalyzed hydrodefluorination of fluoroarenes utilizing amide solvent as reductant. *Chem.—Eur. J.* **2021**, *27* (49), 12635−12641.
(86) Ghosh, I.; Marzo, L.; Das, A.; Shaikh, R.; König, B. Visible light mediated photoredox catalytic arylation reactions. *Acc. Chem. Res.* **2016**, *49* (8), 1566−1577.
(87) Mandigma, M. J. P.; Kaur, J.; Barham, J. P. Organophotocatalytic mechanisms: simplicity or naïvety? Diverting reactive pathways by modifications of catalyst structure, redox states and substrate preassemblies. *ChemCatChem.* **2023**, *15* (11), No. e202201542.
(88) Wortman, A. K.; Stephenson, C. R. J. EDA photochemistry: mechanistic investigations and future opportunities. *Chem.* **2023**, *9* (9), 2390−2415.
(89) Yuan, Y. -q.; Majumder, S.; Yang, M.-h.; Guo, S.-r. Recent advances in catalyst-free photochemical reactions via electron-donor-acceptor (EDA) complex process. *Tetrahedron Lett.* **2020**, *61* (8), No. 151506.
(90) Strieth-Kalthoff, F.; Glorius, F. Triplet energy transfer photocatalysis: unlocking the next level. *Chem.* **2020**, *6* (8), 1888−1903.
(91) Schmid, L.; Glaser, F.; Schaer, R.; Wenger, O. S. High triplet energy iridium(III) isocyanoborato complex for photochemical upconversion, photoredox and energy transfer catalysis. *J. Am. Chem. Soc.* **2022**, *144* (2), 963−976.

https://doi.org/10.1021/acs.jpclett.4c00895
J. Phys. Chem. Lett. 2024, 15, 7945−7953

(92) Majek, M.; Faltermeier, U.; Dick, B.; Pérez-Ruiz, R.; Jacobi von Wangelin, A. Application of visible-to-UV photon upconversion to photoredox catalysis: the activation of aryl bromides. *Chem.—Eur. J.* **2015**, *21* (44), 15496−15501.
(93) Bassan, E.; Gualandi, A.; Cozzi, P. G.; Ceroni, P. Design of BODIPY dyes as triplet photosensitizers: electronic properties tailored for solar energy conversion, photoredox catalysis and photodynamic therapy. *Chem. Sci.* **2021**, *12* (19), 6607−6628.
(94) Sartor, S. M.; Chrisman, C. H.; Pearson, R. M.; Miyake, G. M.; Damrauer, N. H. Designing high-triplet-yield phenothiazine donor−acceptor complexes for photoredox catalysis. *J. Phys. Chem. A* **2020**, *124* (5), 817−823.
(95) Thompson, B. J.; Kumar, A.; Huxter, V. M. Concentration-dependent aggregation of methylene blue acting as a photoredox catalyst. *Phys. Chem. Chem. Phys.* **2024**, DOI: 10.1039/D4CP02026J.
(96) McCarthy, B. G.; Pearson, R. M.; Lim, C.-H.; Sartor, S. M.; Damrauer, N. H.; Miyake, G. M. Structure−property relationships for tailoring phenoxazines as reducing photoredox catalysts. *J. Am. Chem. Soc.* **2018**, *140* (15), 5088−5101.
(97) Ma, J.; Xie, X.; Meggers, E. Catalytic asymmetric synthesis of fluoroalkyl-containing compounds by three-component photoredox chemistry. *Chem.—Eur. J.* **2018**, *24* (1), 259−265.

https://doi.org/10.1021/acs.jpclett.4c00895
J. Phys. Chem. Lett. 2024, 15, 7945−7953